



# Consistent floor response spectra for performance-based seismic design of nonstructural elements

Roberto J. Merino<sup>1</sup> | Daniele Perrone<sup>1</sup> | Andre Filiatrault<sup>1,2</sup>

<sup>1</sup>University School for Advanced Studies IUSS Pavia, Pavia, Italy

<sup>2</sup>Department of Civil, Structural and Environmental Engineering, the State University of New York at Buffalo, Buffalo, NY, USA

## Correspondence

Roberto J. Merino, University School for Advanced Studies IUSS Pavia, Pavia 27100, Italy.

Email: robertojavier.merinovela@iusspavia.it

## Funding information

Italian Department of Civil Protection, Grant/Award Numbers: ReLUIS 2019-2021 Project and ReLUIS 2019-2021; Italian Ministry of Education, University and Research, Grant/Award Number: Dipartimenti di Eccellenza

## Summary

The achievement of adequate performance objectives for buildings under increasing seismic intensities is not only related to the performance of structural members but also to the behavior of nonstructural elements. The need to properly design nonstructural elements for earthquakes has been largely demonstrated in the last few years and has become an important objective within the earthquake engineering community. A crucial aspect in the proper design of nonstructural elements is the definition of the seismic demand in terms of both absolute acceleration and relative displacement floor response spectra. In the first part of this study, relative displacement and absolute acceleration floor response spectra were computed for four reinforced concrete moment-resisting archetype frames via dynamic time-history analyses and were compared with floor response spectra predicted by means of two recent simplified methodologies available in the literature. It was observed that one of the existing methodologies is generally unable to predict consistent absolute acceleration and relative displacement floor response spectra. An improved procedure is developed for estimating consistent floor response spectra for building structures subjected to low and medium-high seismic intensities. This new procedure improves the predictions of a relative displacement floor response spectrum by constraining its ordinates at long nonstructural periods to the expected peak absolute displacement of the floor. The resulting acceleration and relative displacement response spectra are then consistently related by the well-known pseudo-spectral relationship over the entire nonstructural period range. The effectiveness of the proposed methodology was appraised against floor response spectra computed from nonlinear time-history analyses.

## KEYWORDS

floor response spectra, nonstructural elements, nonstructural components, seismic demand

## 1 | INTRODUCTION

Recent advancements in performance-based earthquake engineering have pointed out the importance of the seismic design of nonstructural elements (NSEs) in buildings. Damage observed during the past earthquakes that have struck densely built regions,<sup>1-3</sup> as well as recent loss estimation studies,<sup>4,5</sup> indicate that NSEs significantly affect the immediate functionality and economic losses in typical buildings. For example, Miranda et al<sup>1</sup> described the damage that occurred

at the Santiago International Airport following the 2010 Chile earthquake. The airport terminal did not suffer any significant structural damage but was closed for several days because of severe damage to pressurized fire suppression sprinkler piping systems interacting with ceiling systems.<sup>1</sup> During the same earthquake, four hospitals completely lost their functionality, and over 10 more lost 75% of their functionality because of damage to sprinkler piping systems.<sup>1</sup> Similarly, post-earthquake surveys carried out by Perrone et al<sup>2</sup> following the 2016 Central Italy earthquake identified damage to NSEs in important facilities such as city halls, factories, hospitals and schools. Major damage was reported to ceiling systems, partitions, piping systems, and shelves. The importance of NSEs is highlighted by the FEMA P-58 seismic loss estimation methodology<sup>6</sup> that explicitly considers the contributions of NSEs to the expected losses. A recent study dealing with the seismic loss assessment of school buildings in Italy reported that for reinforced and prestressed concrete school buildings, up to 80% of earthquake related losses might be associated to NSEs.<sup>4</sup>

NSEs are generally divided into two main categories for damage assessment and design purposes: displacement sensitive and acceleration sensitive. For displacement-sensitive NSEs, the damage is mainly related to the inter-story drifts in the supporting structure. Typical examples of displacement-sensitive NSEs are wall partitions and glazing facades. The damage induced in acceleration-sensitive NSEs is mainly due to the overturning or excessive displacements relative to the supporting structure caused by inertia forces arising from horizontal and vertical floor accelerations. Examples of acceleration-sensitive NSEs are piping systems, ceiling systems and anchored or free-standing mechanical equipment. Seismic provisions in modern building codes deal with the seismic design of displacement-sensitive NSEs by imposing inter-story drift limits to the supporting structures, while the performance of acceleration-sensitive NSEs is verified using simplified force-based approaches that calculate design inertia forces to be applied at the center of mass of the NSEs.<sup>7,8</sup> To overcome the shortcomings of the force-based seismic design approaches, Filiatrault et al<sup>9</sup> recently proposed a direct displacement-based design (DDBD) procedure similar to the DDBD methodology originally proposed for structures.<sup>10</sup> The methodology applies to NSEs attached to a single location in the supporting structure and for which damage is the result of excessive displacements relative to the supporting structure. One of the key aspects of this DDBD methodology is the definition of the seismic demand in terms of relative displacement floor response spectra (FRS). In addition, current seismic code design provisions for NSEs require the calculation of the relative displacements of NSEs relative to the supporting structure to provide sufficient clearance and avoid undesirable interactions between NSEs and structural elements. A simple methodology capable of accurately predicting relative displacement FRS would be a powerful tool to improve the seismic design of NSEs.

In the last few years, significant efforts have focused on the evaluation of the acceleration demand on NSEs in typical structural typologies. Lin and Mahin<sup>11</sup> and Sewell et al<sup>12</sup> conducted pioneering works in the evaluation of peak floor accelerations in yielding structures. Sewell et al<sup>12</sup> demonstrated that the amplification of FRS peaks is influenced by the localized nonlinear behavior occurring in the supporting structure. Medina et al<sup>13</sup> studied peak floor accelerations and FRS for light NSEs mounted in regular moment-resisting frames and concluded that seismic code provisions do not always provide adequate estimations of peak floor accelerations. In addition, the modal properties and the yielding of the supporting structure significantly influence FRS, with the latter reducing the maximum expected demand on NSEs. Sankaranarayanan and Medina<sup>14</sup> studied the main factors that caused amplification or reduction in FRS ordinates and concluded that the peak acceleration experienced by an NSE is strongly related to its location in the building, the ratio between its period and the period of the building, its damping ratio, and the level of inelastic response exhibited by the supporting structure. Chaudhuri and Villaverde<sup>15</sup> and Chaudhuri and Hutchinson<sup>16</sup> stated that an amplification of peak spectral acceleration because of building nonlinearity could occur when the NSEs are located at the lower floors of a building and the NSEs are tuned to one of its higher modes. A correlation with the ground motions characteristics was also observed.

To improve code prescriptions for NSEs,<sup>7,8</sup> some authors have proposed more accurate methodologies to predict FRS for Single degree-of-freedom (SDOF) and multi degree-of-freedom (MDOF) systems. Miranda and Taghavi<sup>17</sup> proposed an approximate method to estimate floor acceleration demands in multistory buildings responding elastically or quasi-elastically.<sup>17</sup> Singh et al<sup>18,19</sup> proposed two different formulas to evaluate the seismic forces on rigid and flexible NSEs. Politopoulos and Feau<sup>20</sup> investigated the influence of the nonlinear behavior of the supporting structure on acceleration FRS by means of simplified models. Politopoulos<sup>21</sup> extended the previous study to MDOF nonlinear structures and concluded that, generally, nonlinearity has a beneficial effect on FRS. More recently, Petrone et al<sup>22</sup> proposed a methodology to construct FRS for European buildings designed according to Eurocode 8 prescriptions<sup>8</sup> and subjected to frequent (serviceability level) earthquake ground motions. Likewise, Vukobratović and Fajfar<sup>23</sup> proposed a simple methodology to construct FRS that was calibrated both for elastic and inelastic supporting structures. The methodology highlights the significant influence of higher modes on FRS. Similar considerations were introduced in the methodology

recently developed by Sullivan et al.<sup>24</sup> This methodology was originally proposed for linear and nonlinear SDOF structures and was recently extended to nonlinear MDOF systems.<sup>24–26</sup>

Despite the significant efforts to develop simple methodologies to predict absolute acceleration FRS, relative displacement FRS have received almost no attention. To the author's knowledge, only two recent studies deal with the prediction of the seismic demand for NSEs in terms of relative displacements.<sup>27,28</sup> Obando and Lopez-Garcia<sup>27</sup> characterized inelastic displacement ratios of inelastic acceleration-sensitive nonstructural components subjected to floor accelerations. Calvi<sup>28</sup> proposed a methodology to predict relative displacement FRS. In particular, Calvi further developed the work by Sullivan et al.<sup>24,25</sup> by applying some of their concepts to the prediction of relative displacement FRS for nonlinear SDOF supporting structures. The methodology provides expressions that are valid in a range of nonstructural periods up to the fundamental period of the supporting structure followed by constant spectral displacements for longer nonstructural periods. This approach would lead to inaccuracy when designing or assessing NSEs with periods longer than the period of the supporting structure, such as pendant lighting fixtures, steel storage-racks, vibration isolated mechanical equipment, or important artworks that could be seismically base isolated.<sup>29–31</sup> The recent “recommendations for improved seismic performance of nonstructural components” developed by the National Institute of Standards and Technology (NIST)<sup>32</sup> provides some statistical data on the ratios between the fundamental periods of NSEs and of supporting structures. For flexible NSEs attached to a supporting structure having a fundamental period equal to 0.3 seconds, the probability that the period of a NSE be longer than the fundamental period of the supporting structure is approximately 45%, while for a supporting structure having a fundamental period equal to 0.85 seconds, the corresponding probability is 15%. There is a need to better define relative displacement FRS for the seismic design and assessment of NSEs characterized by periods longer than the fundamental period of the supporting structure.

Based on these considerations, and in order to develop an effective methodology to be used for the application of displacement-based seismic design and assessment of NSEs,<sup>9,33</sup> this study focuses on the development of a simple code-oriented methodology able to provide compatible relative displacement and absolute acceleration FRS. The proposed method modifies the Sullivan et al.<sup>24–26</sup> methodology focusing on reinforced concrete (RC) moment-resisting frames. The effectiveness of the proposed changes was appraised through the results of dynamic nonlinear time-history (NLTH) analyses.

## 2 | PREDICTIONS OF FRS

Significant efforts have been made in recent years to develop simple code-oriented methodologies able to predict, with reasonable accuracy, absolute acceleration FRS in RC and steel buildings. The most recent methodologies<sup>23–26</sup> consider four essential factors affecting absolute acceleration FRS (Figure 1):

1. The influence of the dynamic filtering offered by the vibration modes of the supporting structure. If the natural period of the NSE ( $T_a$ ) is close to the natural period of the supporting structure ( $T_i$ ), an amplification of the spectral acceleration demand occurs (Figure 1C). On the other hand, a de-amplification of the acceleration demand is observed for increasing difference between  $T_a$  and  $T_i$ , with the acceleration spectrum of the ground itself being a lower limit.

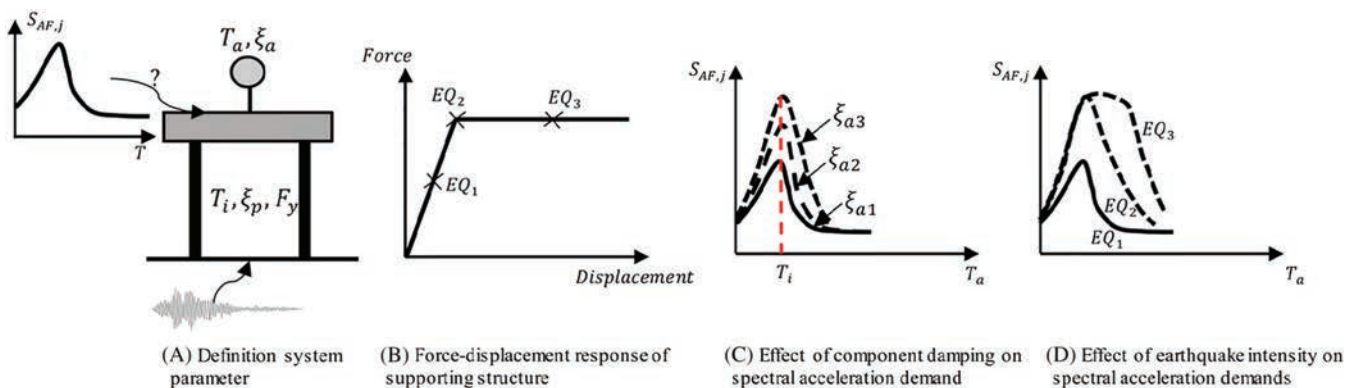


**FIGURE 1** Overview of the main factors affecting absolute acceleration floor response spectra<sup>22</sup> [Colour figure can be viewed at [wileyonlinelibrary.com](http://wileyonlinelibrary.com)]

2. The influence of damping characteristics of the NSEs. As illustrated in Figure 1C, the spectral accelerations affecting the NSEs are significantly influenced by the effective damping of NSEs. Increasing the effective damping causes a reduction in the acceleration demand on NSEs. Ignoring this aspect is one of the main shortcomings of current code provisions and several simplified procedures.
3. The influence of the inelastic response of the supporting structure. For low seismic intensity, with a SDOF supporting structure responding mainly in the elastic range, the absolute acceleration FRS is characterized by a single peak that lies at the fundamental period of the supporting structure. If the seismic input intensity increases and the maximum strength of the supporting structure is mobilized through inelastic response (Figure 1B), the maximum floor spectral acceleration is capped by the lateral force capacity of the supporting structure. This peak, however, extends into a plateau over a wider range of periods because the effective stiffness of the supporting structure degrades, and its effective period lengthens (Figure 1D).
4. Finally, the response of the NSEs should be also taken into account. The inelastic response of the NSEs, in particular in the resonance region, could significantly affect the prediction of the FRS.

The most recent methodologies proposed by Sullivan et al<sup>24-26</sup> and Vukobratović and Fajfar<sup>23</sup> to predict absolute acceleration response spectra, which are the focus of this paper, consider the above factors,<sup>34,35</sup> as described below.

## 2.1 | The Sullivan et al methodology

The methodology originally proposed by Sullivan et al<sup>24</sup> to predict absolute acceleration FRS of nonlinear SDOF systems was extended by Calvi and Sullivan to linear elastic MDOF structures<sup>25</sup> and was further modified by Welch and Sullivan<sup>26</sup> to account for nonlinear response of MDOF structures. The first step of the procedure consists in performing an eigenvalue analysis of the supporting structure in order to evaluate its elastic natural periods and mode shapes. Using the results of the eigenvalue analysis and the design ground response spectrum, the peak acceleration for mode  $i$  at floor  $j$  of the supporting structure,  $a_{i,j}$ , is calculated using basic dynamic analysis<sup>36</sup> as follows:

$$a_{i,j} = \phi_{i,j} \Gamma_i \left( \frac{S_A(T_i, \xi_p)}{R_i} \right), \quad (1)$$

where  $\phi_{i,j}$  is the mode shape for mode  $i$  at floor  $j$ ,  $\Gamma_i$  is the participation factor for mode  $i$ ,  $\xi_p$  is the inherent damping of the supporting structure, and  $S_A(T_i, \xi_p)$  is the design ground spectral acceleration associated to mode  $i$  and damping ratio  $\xi_p$ .  $R_i$  in Equation (1) represents the modal reduction factor of the spectral peak of mode  $i$  that can be approximated by:<sup>26</sup>

$$R_i = \mu^{\alpha_i}, \quad (2)$$

where  $\mu$  is the ductility demand on the supporting structure evaluated according to a rational procedure such as the displacement-based assessment method<sup>10</sup> or the N2 methodology.<sup>37</sup> The exponent  $\alpha_i$  in Equation (2) depends on mode  $i$  and on the structural typology of the supporting structure. Welch and Sullivan<sup>26</sup> recommended values of  $\alpha_i$  for steel moment-resisting frames:  $\alpha_i = 1.0$  for the first mode and  $\alpha_i = 0.6$  for higher modes. Additionally, Welch and Sullivan<sup>26</sup> suggested considering the first four vibration modes when the supporting structure has less than eight stories and the first five modes for supporting structures with more than eight stories.

The following set of equations is then used to compute the contribution of each mode to the absolute acceleration FRS:

$$S_{AF\ i,j}(T_a) = \left( \frac{T_a}{T_i} \right)^2 [a_{i,j}(DAF_{\max} - 1)] + a_{i,j} \quad \text{for } T_a < T_i, \quad (3)$$

$$S_{AF\ i,j}(T_a) = DAF a_{i,j} \quad \text{for } T_i \leq T_a \leq T_{e,i}, \quad (4)$$

$$S_{AF\ i,j}(T_a) = a_{i,j} \left[ \left( 1 - \frac{T_a}{T_{e,i}} \right)^2 + (0.5\xi_p + \xi_a) \right]^{-0.667} \quad \text{for } T_a > T_{e,i}, \quad (5)$$

where  $S_{AFi,j}(T_a)$  is the floor spectral acceleration calculated for mode  $i$  at floor  $j$  for an NSE with a fundamental period equal to  $T_a$ ,  $T_i$  is the  $i$ th elastic period of the supporting structure,  $a_{i,j}$  is the peak floor acceleration for mode  $i$  at floor  $j$  (Equation 1),  $DAF$  represents the dynamic amplification factor,  $T_{e,i}$  is the  $i$ th effective period of the supporting structure, while  $\xi_a$  is the equivalent damping ratio of the NSE. For RC frames, the effective period for mode  $i$ ,  $T_{e,i}$ , is evaluated by:

$$T_{e,1} = T_1 \sqrt{\mu}, \quad (6)$$

$$T_{e,i} = T_i \quad \text{for } i \geq 2. \quad (7)$$

If the supporting structures remains in the elastic range, its effective periods are equal to its elastic periods ( $T_{e,i} = T_i$  for all modes  $i$ ), and the FRS is calculated only using Equations (3) and (5). Welch and Sullivan<sup>26</sup> proposed the following three equations to estimate the dynamic amplification factor,  $DAF$ , taking into account both the inherent damping ratio of the supporting structure and of the NSE:

$$DAF_{\max} = \left(0.5\xi_p + \xi_a\right)^{-0.667}, \quad (8)$$

$$DAF = DAF_{\max} \left(0.55 + 0.45 \frac{T_i}{T_B}\right) \quad \text{for } T_i \leq T_B, \quad (9)$$

$$DAF = DAF_{\max} \quad \text{for } T_i > T_B, \quad (10)$$

in which  $T_B$  is the period that marks the start of the constant acceleration region of the design ground acceleration spectrum.<sup>7,8</sup>

Finally, the absolute acceleration FRS for the upper floors (floors located above the mid-height of the supporting structure) are obtained by computing the square root sum of the squares (SRSS) of the modal spectral ordinates at each period (Equations 3-5). For the lower floor levels, the absolute acceleration FRS is obtained by taking the envelope of the ground acceleration response spectrum and the spectral acceleration obtained using the same procedure used for the upper floors.

## 2.2 | The Vukobratović and Fajfar methodology

Inspired by the work of Yasui et al,<sup>38</sup> Vukobratović and Fajfar<sup>23,34,35</sup> proposed a procedure to estimate absolute acceleration FRS for both linear and nonlinear MDOF structures. The method requires to perform an eigenvalue analysis to compute the modal properties of the supporting structure and to apply the N2 method<sup>37</sup> to estimate the response modification factor,  $R_\mu$ , which is related to the ductility demand on the supporting structure. The absolute acceleration FRS for mode  $i$  at floor  $j$ ,  $S_{AF i,j}$ , is estimated by:

$$S_{AF i,j} = \frac{\Gamma_i \phi_{i,j}}{|(T_a/T_i)^2 - 1|} \sqrt{\left(\frac{S_{ep,i}}{R_\mu}\right)^2 + \{(T_a/T_i)^2 S_{es}\}^2}, \quad (11)$$

with

$$S_{AF i,j} \leq AMP_i \Gamma_i \phi_{i,j} \frac{S_{ep,i}}{R_\mu}, \quad (12)$$

where  $S_{ep,i}$  is the elastic spectral acceleration at the  $i$ th period of the supporting structure associated to the inherent damping ratio of the supporting structure and obtained from the elastic ground acceleration response spectrum at the site of interest. On the other hand,  $S_{es}$  is the same elastic ground acceleration response spectrum at the level of damping of the NSE ( $\xi_a$ ) defined for all the nonstructural period range. In other words, while  $S_{ep,i}$  is a constant value,  $S_{es}$  varies with nonstructural period. All the other variables were already defined previously. Finally,  $AMP_i$  in Equation (12) is the acceleration amplification of the floor spectrum related to  $i$ th mode of the supporting structure and given by:

$$AMP_i = 2.5 \sqrt{\frac{10}{(5 + \xi_a)}} \quad \text{for } \frac{T_i}{T_C} = 0, \quad (13)$$

$$AMP_i = \text{linear between } AMP_i \left( \frac{T_i}{T_C} = 0 \right) \text{ and } AMP_i(T_i/T_C > 0.2) \quad \text{for } 0 \leq \frac{T_i}{T_C} \leq 0.2, \quad (14)$$

$$AMP_i = \frac{10}{\sqrt{\xi_a}} \quad \text{for } T_i/T_C > 0.2, \quad (15)$$

where  $T_C$  is the upper limit of the constant spectral acceleration branch of the ground spectrum prescribed by CEN<sup>8</sup> and based on the soil type at the site. To calculate  $S_{AF\ i,j}$ , Equation (11) is applied in the off-resonance region while Equation (12) is used for the resonance region. According to Vukobratović and Fajfar,<sup>34</sup> the resonance region roughly falls in the range  $0.8T_i < T_a < 1.25T_i$ . However, the boundaries of the resonance region are not fixed and are determined automatically by taking into account the upper limit imposed by Equation (12). Despite not being explicitly stated in the original methodology proposed by Vukobratović and Fajfar, it is suggested to account for a lower limit in the generation of the absolute acceleration FRS; this limit is represented by the ground spectrum.<sup>39</sup> In this work, this limit was applied to the floors in the lower half of the supporting structure as recommended in Calvi and Sullivan.<sup>25</sup> Note that if the inelastic behavior of the supporting structure is to be accounted for, its first inelastic mode shape, as determined using the N2 method, should replace the first elastic mode of the structure and the effective period  $T_{e,1}$  (Equation 6) should replace  $T_1$  in Equations (11) through (15). Once the contribution of each mode to the absolute acceleration FRS is defined, these modal contributions are combined to predict the final absolute acceleration FRS. Vukobratović and Fajfar<sup>23,35</sup> recommend using the SRSS combination for nonstructural periods between zero and the period marking the end of the resonance region of the first mode. Beyond this limit, the algebraic sum of each contribution, taking into account the sign of the mode shape values ( $\phi_{i,j}$ ), should be used.

### 2.3 | Limitations of available methodologies

The methodologies proposed by Sullivan et al<sup>24-26</sup> and Vukobratović and Fajfar<sup>23,34,35,39</sup> both provide reasonable estimates of absolute acceleration FRS but do not provide any indication on the predictions of relative displacement FRS. To calculate the relative displacement FRS starting from an absolute acceleration FRS,  $S_{AF}$ , the pseudo-spectral relationship can be used<sup>36</sup>:

$$S_{DF} = \frac{T_a^2}{4\pi^2} S_{AF} g, \quad (16)$$

in which  $S_{DF}$  is the relative spectral displacement at a nonstructural period  $T_a$  and  $g$  is the acceleration of gravity. The direct application of Equation (16) to estimate the relative displacement FRS using the Vukobratović and Fajfar methodology would lead to increasing relative displacements in the resonance region of the FRS. To overcome this issue, a plateau, similar to the one applied to the prediction of the absolute acceleration FRS, is also assumed for the relative displacement FRS. The peak of the relative displacement FRS is computed by applying Equation (16) at the resonance point and then using this as an upper limit for the spectral values.<sup>39</sup> The limitations of the two methodologies in predicting absolute acceleration and relative displacement FRS are highlighted here through an illustrative example. The top floor absolute acceleration and relative displacement FRS of a four-story RC moment-resisting frame were evaluated through NLTH analyses using an ensemble of 20 historical ground motions representative of a medium-high seismic zone in Italy. The median FRS obtained through NLTH analyses were compared with those predicted by the two simplified methodologies. All the details on the analyzed RC frame and the ground motion ensemble are provided in the next section. A serviceability seismicity level, with a 70-year return period, was considered for this illustrative example so that the RC frame remained in the elastic range for all 20 ground motions. Figure 2 compares the absolute acceleration (Figure 2A) and relative displacement (Figure 2B) FRS predicted by the Vukobratović and Fajfar and Sullivan et al methodologies with the median top floor absolute acceleration and relative displacement FRS obtained from the NLTH analyses (assuming a nonstructural damping ratio equal to 5%).

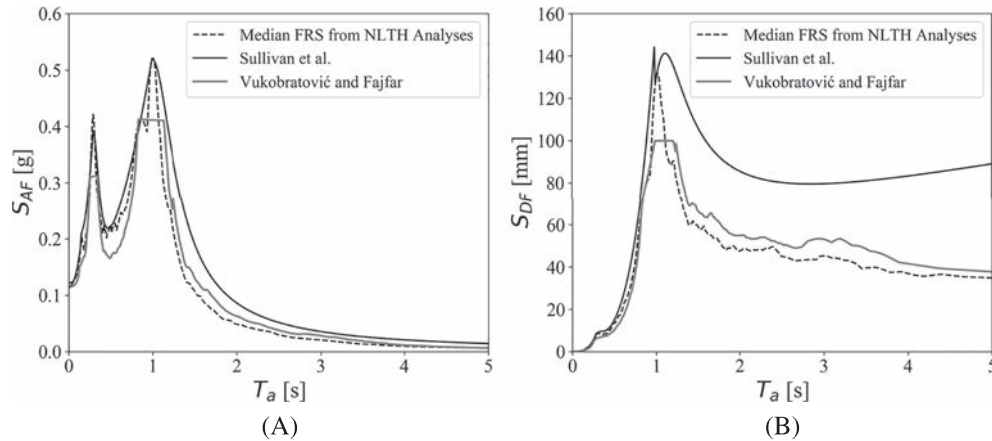


**FIGURE 2** Comparison between FRS predicted by the Vukobratović and Fajfar and Sullivan et al methodologies with median FRS obtained from NLTH analyses on a four-story RC frame: (A) absolute acceleration FRS and (B) relative displacement FRS. FRS, floor response spectra; NLTH, nonlinear time-history; RC, reinforced concrete

As shown in Figure 2, the shapes of both median absolute acceleration and relative displacement FRS are predicted reasonably well by the Vukobratović and Fajfar methodology. This is not surprising considering that it is based on the spectral shape proposed by Yasui et al.<sup>38</sup> obtained by using the Duhamel integral to directly integrate the equations of motion for SDOF systems. However, the peak spectral absolute accelerations and relative displacements at the modal periods of the supporting structure are under-predicted. One of the reasons why the Vukobratović and Fajfar methodology underestimates the spectral values in the resonance region is because it implicitly includes a broadening of the spectral peaks, which is generally combined with a reduction of peak values of about 15%.<sup>39,40</sup> It is also important to note that the peak values strongly depend on the period of the supporting structure and of the NSE as well as on the characteristics of the ground motion.

Figure 2 also shows the comparison between the top floor median FRS obtained from NLTH analyses and the FRS predicted by the Sullivan et al methodology. A good agreement is observed in terms of absolute acceleration FRS both in terms of shape and peak spectral absolute accelerations at the modal periods of the supporting structure. Slightly conservative spectral accelerations are predicted for periods longer than the fundamental period of the supporting structure. The evaluation of the relative displacement FRS using the pseudo-spectral relationship exhibit also a good agreement up to the fundamental period of the supporting structure, but much higher spectral relative displacements are predicted for longer nonstructural periods. Equation (5) predicts relative spectral displacements that decrease slightly beyond the fundamental period of the supporting structure and, beyond 2.0 seconds, start to increase without bounds for very long nonstructural periods. This physically inconsistent behavior is related to the limiting values of Equation (5) that consist of a binomial expression raised to the power of a negative fraction.

The results of this illustrative example show that the methodology proposed by Vukobratović and Fajfar seems to provide consistent absolute acceleration and relative displacement FRS shapes. The methodology proposed by Sullivan et al, on the other hand, seems to provide slightly less consistent absolute acceleration and relative displacement FRS shapes and would benefit from some modifications. The introduction of simple physical-based rules, for example, could lead to consistent absolute acceleration and relative displacement FRS by keeping the simplicity of the methodology. With this in mind, the methodology proposed by Sullivan et al was modified in this study.

### 3 | ARCHETYPE FRAMES

The modifications to the methodology proposed by Sullivan et al,<sup>24-26</sup> in order to better predict consistent absolute acceleration and relative displacement FRS, needed to be carried out and appraised using realistic archetype buildings. For this purpose, the results of NLTH analyses carried out on four RC archetype frames were used to define physical-based rules/modifications to be applied to the Sullivan et al methodology. The RC frames were taken from an extensive database representative of the Italian RC building stock,<sup>41</sup> in which the geometrical and mechanical properties of the buildings were randomly generated assuming the typical variability observed in Italy.

### 3.1 | Description of archetype frames and numerical modelling

The four archetype RC frames are assumed part of different symmetrical moment-resisting RC frame buildings. The buildings are assumed to be located in a site near Cassino (Italy), which is characterized by a peak ground acceleration on firm soil equal to 0.21 g (for a return period of 475 years). The RC frames (Figure 3) were designed according to the Italian Building Code<sup>42</sup> with a ductility class B (the force reduction factor is assumed to be 3.75). Table 1 lists the main geometrical and mechanical properties of the four archetype RC frames. The number of stories ( $S$ ) varies between 2 and 8, while the number of bays ( $B$ ) is assumed equal to 4 or 6. The length of the bays ( $L_b$ ) varies between 3.25 and 3.00 m, while the height of the stories ( $H_s$ ) varies between 2.75 and 3.25 m. The concrete compressive strength ( $f'_c$ ) and reinforcing steel yield strength ( $f_y$ ) were varied in the typical ranges observed in the Italian building stock, as reported in Table 1. Different typologies of building usage were also simulated by varying the live loads on the beams ( $q_k$ ).

To simplify the seismic design of the archetype RC frames, the section of the beams was kept constant at all stories and the columns were not tapered. Table 2 lists the geometrical properties of the beams and columns.

The numerical models of the archetype RC frames were developed using the open source software OpenSees.<sup>43</sup> A lumped plasticity approach was used when modelling the beams and columns. Fiber sections were assigned in locations of possible plastic hinges (ie, extreme ends of the elements). Elastic sections were given a reduced moment of inertia in order to simulate the initial cracking of the concrete.<sup>8</sup> The fiber sections were discretized using 20 fibers along the depth of the elements and 10 along their width. The constitutive model assumed for the steel reinforcement was the Steel01 material in OpenSees, while the Concrete01 material was assigned to the concrete. The material properties of the confined concrete (peak compressive strength and strain at peak strength) were determined using the recommendations given by Priestley et al,<sup>10</sup> while the ultimate compressive strain was assumed as five times the compressive strain at peak strength.<sup>43</sup> The effects of the floor concrete slabs were taken into account by enforcing a rigid diaphragm constraint for all the nodes of each story. The gravity loads were introduced in the models through distributed loads on the beams. Nonlinear geometric effects because of large displacements were considered by assigning the P- $\Delta$  geometric transformation to the columns. Rayleigh tangent stiffness proportional viscous damping was introduced in the numerical models with 5% of critical damping specified in the first two elastic modes of vibration of each frame.

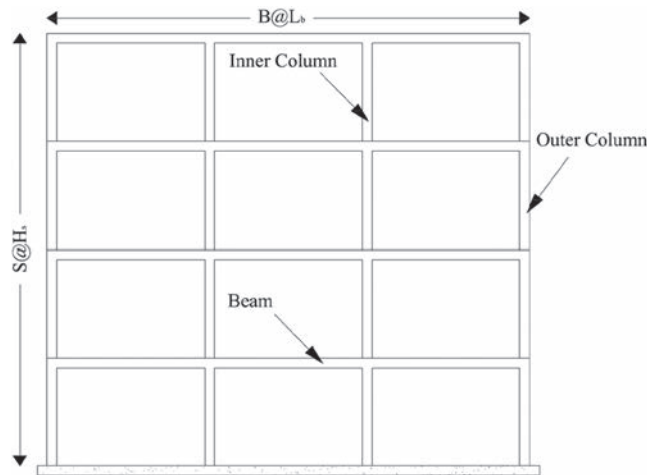


**FIGURE 3** Geometrical configuration archetype reinforced concrete (RC) frames

**TABLE 1** Main geometrical and mechanical properties of archetype RC frames

ID	Number of Stories	Number of Bays	$L_b$ , m	$H_s$ , m	$f'_c$ , MPa	$f_y$ , MPa	$q_k$ , kN/m
1	2	4	3.25	3.25	32	430	7.3
2	4	4	3.25	2.75	32	430	9.75
3	6	6	3.00	3.00	32	430	9.1
4	8	6	3.00	3.00	30	375	9.1

Abbreviation: RC, reinforced concrete.

**TABLE 2** Geometrical properties of beams and columns in archetype RC frames

ID	RC Beams			RC Inner Columns			RC Outer Columns		
	Geometry, mm	Longitudinal reinforcements	Shear reinforcements	Geometry, mm	Longitudinal reinforcements	Shear reinforcements	Geometry, mm	Longitudinal reinforcements	Shear reinforcements
1	250 × 250	3Φ10 + 3Φ10	Φ8/90 mm	250 × 300	8Φ16	Φ8/90 mm	250 × 250	8Φ16	Φ8/90 mm
2	250 × 250	3Φ12 + 3Φ10	Φ8/90 mm	250 × 350	8Φ20	Φ8/90 mm	250 × 250	8Φ16	Φ8/90 mm
3	250 × 250	4Φ10 + 3Φ10	Φ8/90 mm	250 × 350	8Φ20	Φ8/90 mm	250 × 250	8Φ16	Φ8/90 mm
4	300 × 300	3Φ12 + 3Φ12	Φ8/90 mm	350 × 400	8Φ24	Φ10/90 mm	300 × 300	8Φ16	Φ8/90 mm

Abbreviation: RC, reinforced concrete.

Eigenvalue and pushover analyses were conducted on each of the four archetype RC frames in order to obtain the information required to calculate the FRS according to the two simplified methodologies considered herein. Table 3 lists the elastic modal periods and the mode shapes of the four archetype RC frames. Figure 4 shows the pushover curves (Figure 4A) and the normalized displacement of each story at the maximum base shear capacity of the four archetype RC frames (Figure 4B).

### 3.2 | Hazard and ground motion selections

A site near the city of Cassino, Italy, was chosen for the ground motions selection. This site is characterized by a peak ground acceleration on stiff soil equal to 0.21 g for a 475-year return period.

In order to verify the effectiveness of the Sullivan et al.<sup>24-26</sup> methodology and to develop the required modifications, the ground motion selection was carried out for two seismic intensities representative of return periods equal to 70 and 2475 years. The 70-year return period represents a serviceability seismic intensity level aimed at investigating the elastic response of the archetype RC frames. This is particularly important not only to calibrate the modifications in the elastic range but also because the damage to NSEs at low serviceability level seismic intensities often controls the expected annual economic losses suffered by buildings. The 2475-year return period is considered as maximum considered earthquake intensity level according to the Italian seismic provisions for residential buildings. The conventional design return period equal to 475 years was considered only for design purposes and was not taken into account in the numerical analyses because the archetype RC frames did not exhibit significant inelastic responses at that design intensity (the required strength of the frames was controlled by gravity loads).

Twenty historical ground motion records were selected from the PEER NGA-West database.<sup>44</sup> The geometric means of the record pairs were selected to match the conditional mean spectrum according to the methodology proposed by Jayaram et al.<sup>45</sup> Only the first component of each record pair was considered in the analyses. Figure 5 shows the median and individual response spectra of all 20 selected ground motions, in the spectral acceleration ( $S_a$ )-spectral displacement ( $S_d$ ) response spectrum (ADRS) format, for the 70-year (Figure 5A) and 2475-year (Figure 5B) return periods assuming a conditional period equal to 1.0 second and a damping ratio ( $\xi_p$ ) equal to 5%. The spectral acceleration ( $S_a$ ) at 1.0 second was retrieved from the hazard curve at the site and was found to be 0.075 and 0.67 g for a return period equal to 70 and 2475 years, respectively.

## 4 | IMPROVED METHODOLOGY TO PREDICT CONSISTENT RELATIVE DISPLACEMENT AND ABSOLUTE ACCELERATION FRS

The methodology proposed by Sullivan et al.<sup>24-26</sup> is modified in this study in order to predict consistent absolute acceleration and relative displacements FRS. The main issue with this procedure for the prediction of relative displacement FRS lies in Equation (5), which is transformed through the pseudo-spectrum relationship to predict the FRS for non-structural periods longer than the supporting structure's effective period. Sullivan et al.<sup>24,26</sup> derived this equation by empirically modifying the form for the dynamic amplification of a shock spectrum for an undamped SDOF system. This formulation provides a theoretical basis to the equation but is not consistent when relative displacement FRS are calculated. From a physical point of view, the relative displacement FRS decreases beyond the effective period of the supporting structure toward the peak floor absolute displacement at very long nonstructural periods. Considering the shape of traditional ground response spectra, it would be natural to assume that the third branch (Equation 5) of the relative displacement FRS (for  $T_a > T_{e,i}$ ) is proportional to  $T_a^n$ , with  $n < 0$  since the spectral displacements should decrease with increasing nonstructural periods. The chosen functional form for the third branch of the relative displacement FRS should be such that when multiplying it by  $4\pi^2/T_a^2$ , it would yield the correct form of the acceleration FRS, which would then be proportional to  $T_a^{n-2}$ , with  $(n-2) < -2$ . According to Equation (3), the first branch of the acceleration FRS varies proportionally to  $T_a^2$ , making the first branch of the relative displacement FRS vary proportionally to  $T_a^4$ . It is proposed here to modify the third branch of the absolute acceleration FRS (Equation 5) in order to make it vary proportionally to  $T_a^{-4}$ . Consequently, the relative displacement FRS will vary proportionally to  $T_a^{-2}$ . The following equation is proposed to predict the spectral displacements,  $S_{DF,i,j}$ , for long periods (ie,  $T_a > T_{e,i}$ ):

$$S_{DF,i,j} = C_1 + \frac{C_2}{T_a^2} \quad \text{for } T_a > T_{e,i}, \quad (17)$$



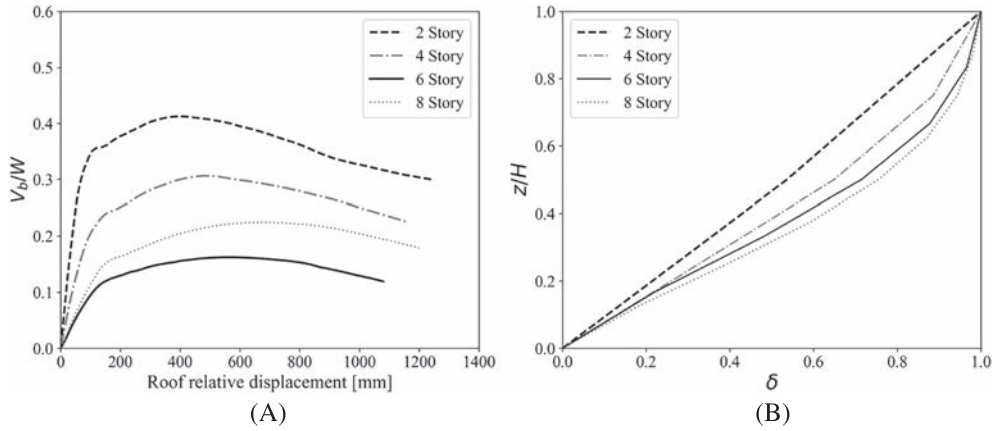


**FIGURE 4** Nonlinear response of the case archetype reinforced concrete (RC) frames: (A) pushover curves in which  $V_b/W$  represents the ratio between the base shear capacity ( $V_b$ ) and the seismic weight ( $W$ ) plotted against the roof relative displacement; (B) normalized displaced shape at the maximum capacity of the RC frames, in which  $z/H$  is the relative elevation along the height of the RC frame and  $\delta$  represents the displacement of each story normalized by the displacement of the roof at maximum base shear

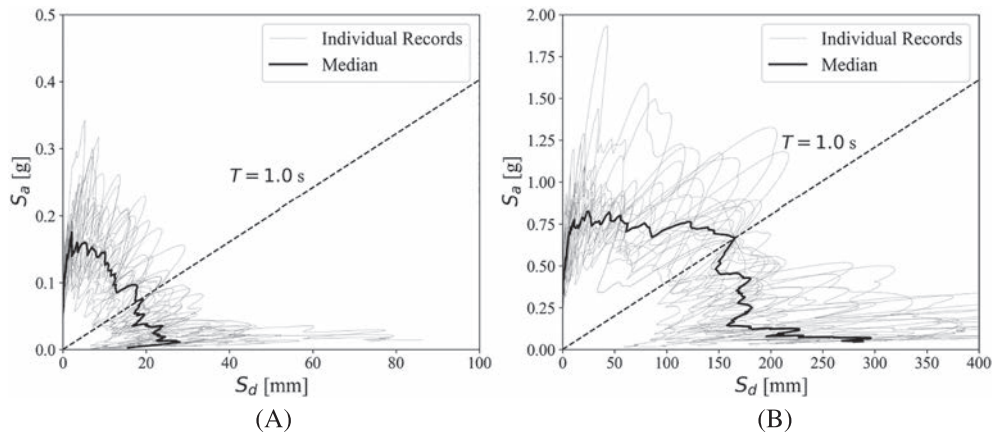


**FIGURE 5** Median and individual response spectra of all 20 selected ground motions, in acceleration-spectral displacement response spectrum (ADRS) format and assuming  $\xi_p = 5.0\%$ , for a conditional period equal to 1.0 second: (A) 70-year return period and (B) 2475-year return period

where  $C_1$  and  $C_2$  are constants determined using two boundary conditions. The first boundary condition is obtained by calculating the value of  $S_{DF,i,j}$  at the effective period,  $T_{e,i}$ , of the supporting structure. As pointed out by Calvi,<sup>28</sup> this value is obtained by Equation (16) for the modal peak floor spectral absolute acceleration ( $S_{AF,i,j,max}$ ), obtained by Equation (4). The second boundary condition is taken as the peak floor absolute displacement for which the relative displacement FRS converges toward at very long nonstructural periods. The value of the peak floor absolute displacement is influenced by both the ground displacement and the relative displacement of the floor. Since the peak relative displacement of the floor has contributions from all the modes of the structure, the peak floor absolute displacement is also composed of contributions from each structural mode. For this reason, a new variable,  $\Delta_{ab,i,j}$ , is defined as the contribution of mode  $i$  to the peak floor absolute displacement of floor  $j$  of the supporting structure. According to these two boundary conditions,  $S_{DF,i,j}$  (for  $T_a = T_{e,i}$ ) =  $(T_{e,i}^2/4\pi^2) S_{AF,i,j,max}$  and  $S_{DF,i,j}$  (for  $T_a = \infty$ ) =  $\Delta_{ab,i,j}$ , the constants  $C_1$  and  $C_2$  in Equation (17) can be solved, and the following equation is obtained for predicting the relative spectral displacements for periods longer than the supporting structure's effective periods:

$$S_{DF,i,j} = \Delta_{ab,i,j} + \left(\frac{T_{e,i}}{T_a}\right)^2 \left(\frac{T_{e,i}^2}{4\pi^2} S_{AF,max,i,j}g - \Delta_{ab,i,j}\right) \text{ for } T_a > T_{e,i}. \tag{18}$$

#### 4.1 | Estimating peak floor absolute displacement in buildings under the serviceability seismic intensity (70-year return period)

The total peak floor absolute displacement,  $\Delta_{ab,j}$ , of floor  $j$  of a supporting elastic structure, subjected to serviceability seismic intensity (70-year return period ground motions in this study) is related to the peak floor relative displacement of the same floor and to the peak ground displacement (PGD). Since the displacement of the ground is generally not perfectly in phase with the relative displacement of the supporting structure, it can be assumed that  $\Delta_{ab,j}$  can be estimated by the SRSS of the PGD and the modal peak floor relative displacements ( $\Delta_{R,i,j}$ ):

$$\Delta_{ab,j} = \sqrt{\sum_{i=1}^n \Delta_{R,i,j}^2 + PGD^2}, \quad (19)$$

in which  $i$  represents the mode shape, while  $j$  is the considered floor. For stiff structures, the floor relative displacement of the supporting structure tends to be more in phase with the ground displacement. Even though Equation (19) is built on the assumption that they are not perfectly in phase, it still produces an accurate estimate of the peak floor absolute displacement because the peak floor relative displacement of stiff structures tends to be small and their peak floor absolute displacement converges to the PGD. The consequence of Equation (19) is that the individual modal contributions ( $\Delta_{ab,i,j}$ ) to the peak floor absolute displacement,  $\Delta_{ab,j}$ , in Equation (18) can be expressed in the following way:

$$\Delta_{ab,1,j} = \sqrt{\Delta_{R,1,j}^2 + PGD^2}, \quad (20)$$

$$\Delta_{ab,i,j} = \Delta_{R,i,j} \quad \text{for } i > 1. \quad (21)$$

These two equations insure that the absolute displacement of floor  $j$ ,  $\Delta_{ab,j}$ , is obtained through an SRSS combination of the modal contributions of the relative displacements of floor  $j$  and the PGD. In other words, the SRSS combinations of Equations (20) and (21) are equal to Equation (19). Equations (20) and (21) assume, for convenience, that the ground displacement affects only the contribution of the first mode to the peak floor absolute displacement. The usefulness of this assumption in estimating consistent FRS will become apparent in Section 4.3. Even though this assumption is made only for practical convenience, in most practical cases, the contributions of the higher modes to peak floor relative displacement, and therefore to the peak floor absolute displacement, are small. The results of NLTH analyses carried out on the four archetype RC frames presented in Section 3 are used to validate Equation (19) (and by extension Equations 20 and 21 since their SRSS combinations produce Equation 19).

##### 4.1.1 | Validation by NLTH analyses

The peak floor absolute displacements predicted by Equation (19) for the four archetype RC moment-resisting frames were compared with those obtained from NLTH analyses under the 70-year ground motions. The predicted peak floor absolute displacements were computed with the results of the modal analysis presented in Section 3 and with the median PGD value obtained from the displacement time-histories of the records shown in Figure 5A (return period of 70 years). Figure 6 shows the comparison between the predicted peak floor absolute displacement values and those obtained from NLTH analyses for three representative floors of the RC frames (first, mid-height, top). Because of space limitation, the results are shown only for the two-, four-, and eight-story frames. In Figure 6, the vertical axis reports the peak floor absolute displacement values obtained from the NLTH analyses ( $\Delta_{ab,NLTH}$ ), while the horizontal axis reports the results obtained from Equation (19) ( $\Delta_{ab,SRSS}$ ) for each of the 20 records. The regression line that best fit the results, in terms of coefficient of determination ( $R^2$ ), is also plotted (dotted line) along with a regression line representing a one-to-one correlation (solid line).

The values of  $R^2$  obtained for the regression line characterized by a slope ( $m$ ) equal to unity (ie, one-to-one correlation) vary from 0.91 to 1.00, with the lowest values obtained at the highest floors. The values of the slopes  $m$  of the best-fit regression lines vary from 0.99 to 1.10 with  $R^2$  varying between 0.93 and 1.00. Even though the estimation of the optimal slope,  $m$ , is associated with a slightly higher correlation than that associated with a slope of unity, Equation (19) provides a very good estimate of the peak floor absolute displacements for the four archetype RC frames considered. In other words, for the analyzed archetype RC frames responding in the elastic range under the 70-year ground motions,

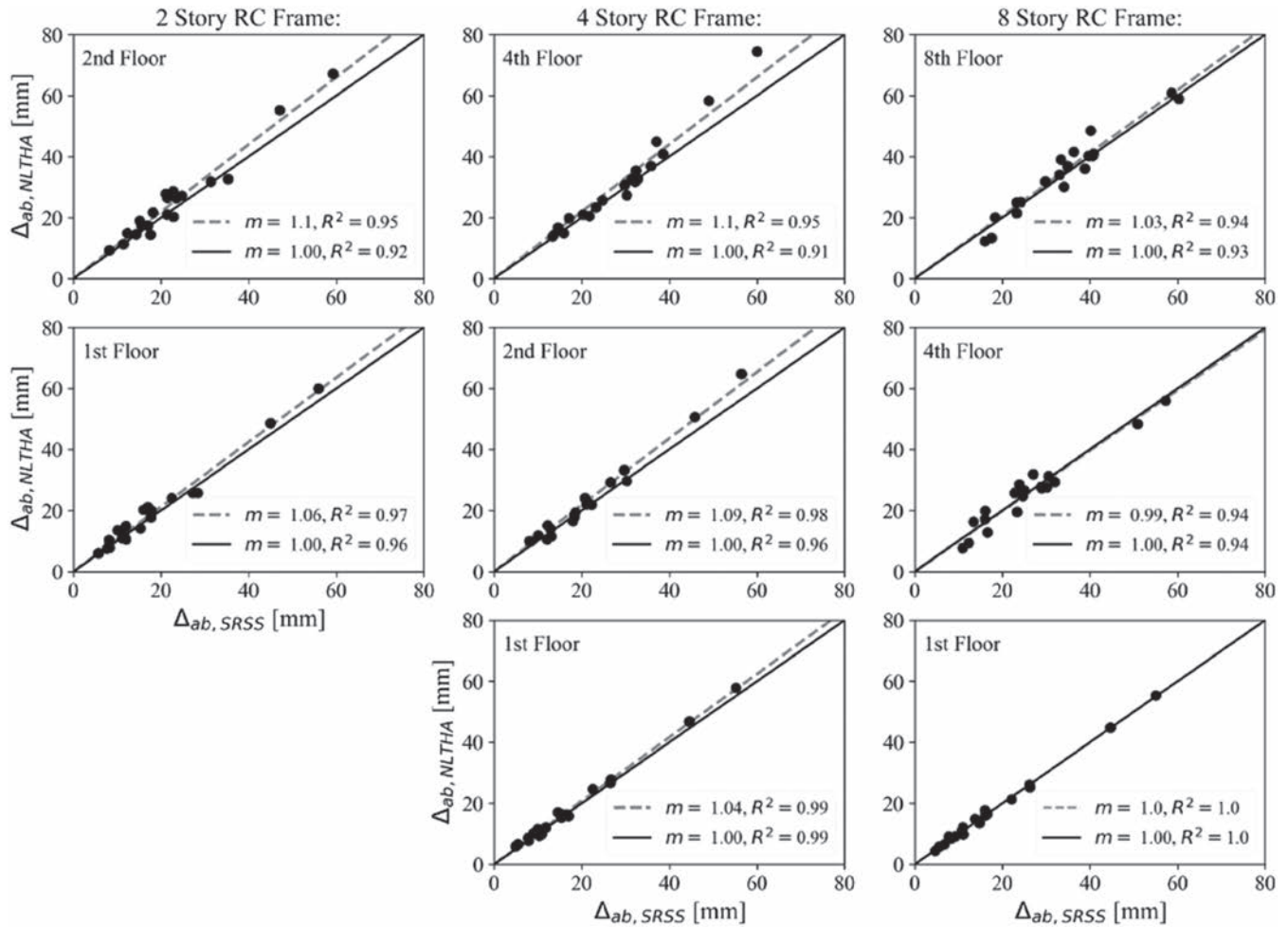


**FIGURE 6** Peak floor absolute displacements from NLTH analyses (vertical axes) and from Equation (19) (horizontal axes) obtained for the two-, four-, and eight-story RC frames (each in one column) under 70-year ground motions. NLTH, nonlinear time-history; RC, reinforced concrete; SRSS, square root sum of the squares

$\Delta_{ab,j}$  can be accurately predicted by performing an SRSS combination between the modal components of the peak floor relative displacement and the PGD.

## 4.2 | Estimating the peak floor relative displacement in buildings under the maximum considered earthquake (2475-year return period)

The prediction of peak floor relative displacements for structures subjected to the 2475-year ground motions requires a more detailed approach to account for the possible inelastic response of the supporting structures. Some methodologies are available in the literature to estimate relative displacements of nonlinear supporting structures.<sup>10,37,46</sup> Even though the N2 methodology allows estimating peak floor relative displacements without any iterations, the Displacement-Based assessment methodology, first proposed by Priestley et al,<sup>10</sup> is used in this study because it produced better results for the specific RC frames analyzed herein. The main steps required to estimate the peak floor relative displacements are listed and briefly described below.

1. The first step requires to compute the capacity (pushover) curve of the supporting structure. The capacity curve is required in order to estimate: the base shear corresponding to the seismic demand ( $V_b$ ), the first inelastic mode shape ( $\delta$ ), and the yield displacement ( $\Delta_y$ ).
2. The second step consists in transforming the MDOF supporting structure into an equivalent linear SDOF system. The effective mass ( $m_e$ ) of the equivalent SDOF system can be calculated by:

$$m_e = \frac{\left(\sum_{j=1}^n m_j \delta_j\right)^2}{\sum_{j=1}^n m_j \delta_j^2}, \quad (22)$$

where  $m_j$  is the mass at the  $j$ th floor of the supporting structure and  $\delta_j$  represents the first inelastic mode shape at the same  $j$ th story, with  $n$  being the number of stories. The first inelastic mode shape should be defined at the maximum base shear capacity of the structure. Note that  $\delta_j$  may change with the displacement demand, although this is usually not the case for supporting structures designed according to modern building standards.<sup>10,37</sup> To convert the MDOF system to an equivalent SDOF system, the yield displacement ( $\Delta_y$ ) of the equivalent SDOF system has to be computed. Assuming that the first inelastic mode shape is representative of the displacement shape at yielding for RC moment-resisting frames, the following equation can be used:

$$\Delta_y = \frac{\sum_{j=1}^n m_j \delta_j^2}{\sum_{j=1}^n m_j \delta_j} \left( \frac{\Delta_{y,n}}{\delta_n} \right), \quad (23)$$

where  $\Delta_{y,n}$  is the roof yield displacement obtained from pushover analysis ( $n$  represents the top floor) and  $\delta_n$  is the value of the inelastic mode shape at the roof (because of how  $\delta$  is normalized here, these values equal to one).

3. The third step consists in defining the seismic hazard for a given seismic intensity. The ground response spectrum should be initially computed for the inherent damping ratio of the supporting structure ( $\xi_p$ ).
4. The fourth step consists in calculating the displacement demand,  $\Delta_d$ , of the equivalent SDOF system when subjected to the ground response spectrum from step 3. The calculation of  $\Delta_d$  requires an iterative procedure. The following steps have to be followed to define  $\Delta_d$ :
  - a. Assume a hypothetical value of  $\Delta_d$ .
  - b. Compute the ductility demand  $\mu$  of the equivalent SDOF system as  $\mu = \Delta_d/\Delta_y$ .
  - c. Compute the equivalent viscous damping,  $\xi_e$ . For RC moment-resisting frames, the equation proposed by Dwairi et al<sup>47</sup> could be used:

$$\xi_e = 0.05 + 0.444 \frac{(\mu - 1)}{\pi \mu}. \quad (24)$$

Dwairi et al<sup>47</sup> calibrated Equation (24) using results of NLTH analyses from a comprehensive parametric study. The equation was corrected to avoid producing the unrealistically high values of equivalent viscous damping computed using the classical equal area approach.

- d. Compute the spectral reduction factor<sup>8</sup>:  $R_\xi = \sqrt{0.07/(0.02 + \xi_e)}$ .
- e. Reduce the ground response spectrum, defined in step 3, by  $R_\xi$ .
- f. Compute the base shear ( $V_b$ ) corresponding to  $\Delta_d$ .
- g. Compute the effective stiffness at the displacement demand as  $K_e = V_b/\Delta_d$ .
- h. Evaluate the effective period as:  $T_e = 2\pi \sqrt{m_e/K_e}$ .
- i. Enter the reduced ground response spectrum with  $T_e$ , and read the corresponding value of  $S_D(T_e, \xi_e)$ . This value is assumed as  $\Delta_d$  for the next iteration. The procedure is repeated until  $\Delta_d$  converges.
- j. The final step involves transforming the results from the equivalent SDOF system to the original MDOF supporting structure. Therefore, the peak floor relative displacements related to the first inelastic mode shape of each of the  $j$ th floors of the supporting structure,  $\Delta_{R,1,j}$ , can be computed as follows:

$$\Delta_{R,1,j} = \frac{\sum_{j=1}^n m_j \delta_j}{\sum_{j=1}^n m_j \delta_j^2} \delta_j \Delta_d \quad (25)$$

Equation (25) considers only the peak floor relative displacements related to the first inelastic mode. The contributions of the higher modes can be simply estimated from an elastic modal response spectrum analysis. According to Priestley et al,<sup>10</sup> the contributions of the higher modes to the overall displacement of a floor are generally negligible.

### 4.2.1 | Validation by NLTH analyses

The inelastic peak floor absolute displacements ( $\Delta_{ab,j}$ ) predicted using Equation (19), and for which  $\Delta_{R,i,j}$  was calculated using the procedure presented in Section 4.2, were compared with those obtained from NLTH analyses under the 2475-year ground motions. The results of the pushover analysis presented in Section 3.1 were used in the iterative procedure required to estimate the peak floor relative displacement of the first mode for the archetype RC frames. Table 4 summarizes the data required to compute  $\Delta_{R,i,j}$  using Equations (22) to (24) and the displaced shapes reported in Figure 4B.

The predicted values of peak floor absolute displacements for supporting structures under the 2475-year ground motions (Figure 5B) are presented in Figure 7 using the same format as for the case of the 70-year ground motions

**TABLE 4** Data required to compute  $\Delta_{R,i,j}$  according to the procedure proposed in Section 4.2 for archetype frames under 2475-year ground motions

	Two Stories	Four Stories	Six Stories	Eight Stories
$m_e$ , kNs <sup>2</sup> /mm	0.06	0.11	0.23	0.30
$\Delta_y$ , mm	62.5	92.7	123.3	147.6
$\Delta_D$ , mm	108.0	129.0	143.0	156.0
$\mu$	1.73	1.39	1.16	1.06
$V_b$ , kN	225	300	320	510

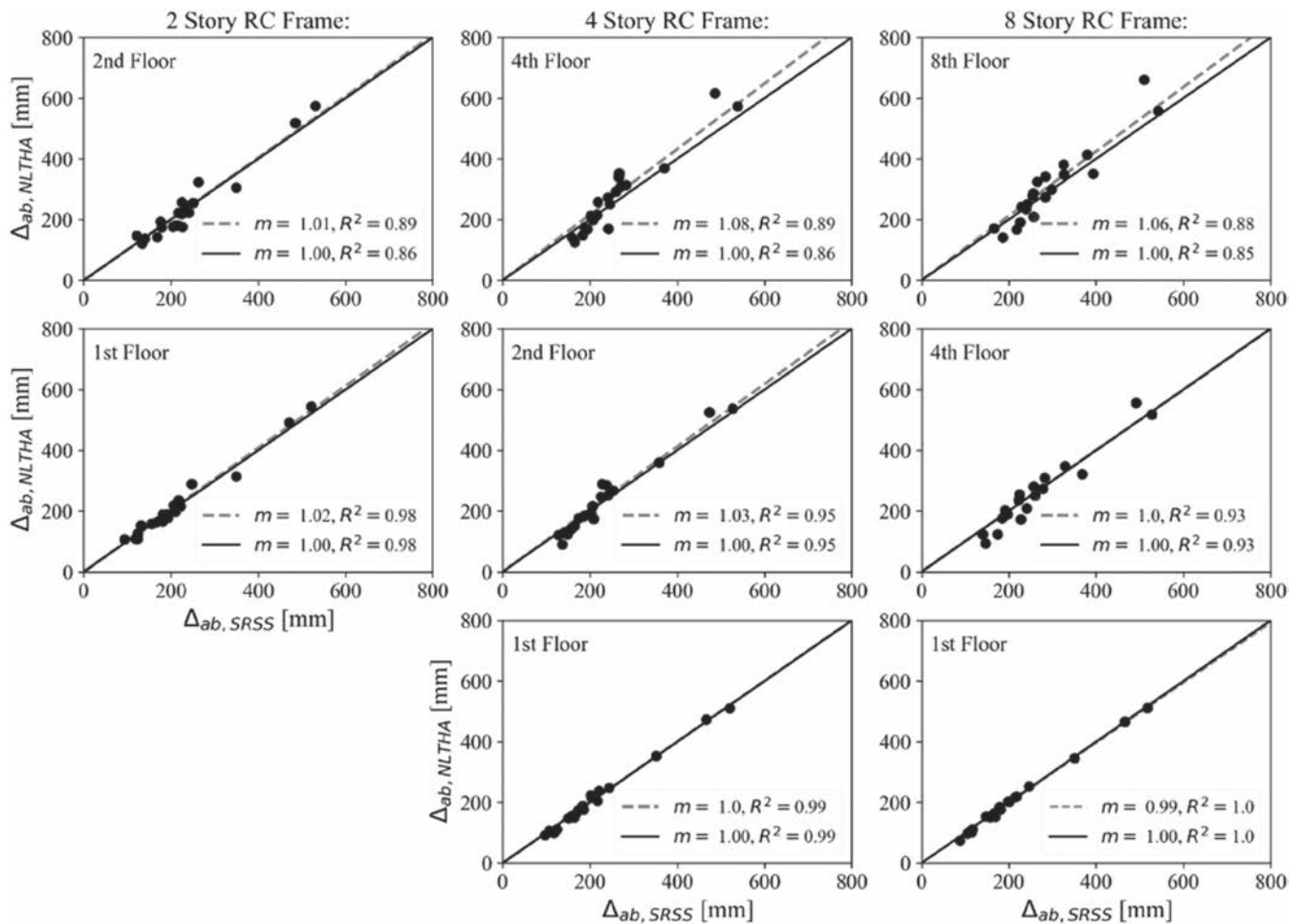


**FIGURE 7** Peak floor absolute displacements from NLTH analyses (vertical axes) and from Equation (19) (horizontal axes) obtained for the two-, four-, and eight-story RC frames (each in one column) under 2475-year ground motions. NLTH, nonlinear time-history; RC, reinforced concrete; SRSS, square root sum of the squares

presented in Figure 6. Again, the  $R^2$  values of a regression line with  $m = 1.0$  and with the best-fit slope are presented in each plot.

From the results shown in Figure 7, Equation (19) is able to predict reasonably well the peak floor relative displacements for the two-, four-, and eight-story frames as demonstrated by the high values of  $R^2$ . The worst predictions by Equation (19) are observed for the top floors of the frames, for which  $R^2$  equals 0.86 and 0.85 respectively. For all the other floors,  $R^2$  is always higher than 0.9. These trends are the results of the peak floor absolute displacements of the lower floors being highly influenced by the ground motions. The responses of the upper floors, on the other hand, are highly influenced by the dynamic response of the structure. The regression lines characterized by the best-fit slopes are also very close to unity, further demonstrating the accuracy of Equation (19) for the archetype RC frames considered.

As expected, the results shown in Figures 6 and 7 indicate that the prediction capability of Equation (19) slightly reduces when considering supporting structures subjected to the 2475-years return period for which nonlinear behavior is observed (see Table 4). This result is due to the fact that the procedure used to predict the peak floor relative displacement relies on empirical relations that are influenced by both the nature of the supporting structure and the nature of the ground motion records. Despite this limitation, the results presented herein demonstrate that Equation (19) is adequate to use as part of the estimation of consistent absolute acceleration and relative displacement FRS within a simplified formulation.

### 4.3 | Summary of the proposed methodology to estimate consistent FRS

This section summarizes the procedure proposed to estimate consistent absolute acceleration and relative displacement FRS for the seismic design and assessment of NSEs. The procedure is general for both structures under low and medium-high seismic intensities. Based on the seismic intensity, and in particular to the expected behavior of the structure (linear/nonlinear), the proposed procedure is slightly different. The procedure consists in the following steps:

1. Perform an eigenvalue analysis of the supporting structure to compute its elastic periods ( $T_i$ ) and mode shapes. Following the recommendations by Welch and Sullivan<sup>26</sup> for RC frames characterized by less than eight stories, the first four modes should be considered, while for RC frames with eight or more stories, the first five modes should be taken into account.
2. Compute the seismic hazard in terms of a ground response spectrum at the damping ratio of the supporting structure ( $\xi_p$ ) for the considered return period.
3. Evaluate the capacity (pushover) curve of the supporting structure. This step is required to determine if the supporting structures yields or not under the seismic hazard level established in step 2.
4. Evaluate the modal contributions to the peak floor acceleration ( $a_{i,j}$ ) and the peak floor relative displacement ( $\Delta_{R,i,j}$ ). The procedure to evaluate these two parameters differs for linear and nonlinear supporting structures. In the case of linear supporting structures,  $a_{i,j}$  and  $\Delta_{R,i,j}$  are evaluated according to the following two equations:

$$a_{i,j} = \frac{\sum_{j=1}^n m_j \phi_{i,j}}{\sum_{j=1}^n m_j \phi_{i,j}^2} \phi_{i,j} S_A(T_i, \xi_p), \quad (26)$$

$$\Delta_{R,i,j} = \frac{\sum_{j=1}^n m_j \phi_{i,j}}{\sum_{j=1}^n m_j \phi_{i,j}^2} \phi_{i,j} S_D(T_i, \xi_p), \quad (27)$$

where  $S_A(T_i, \xi_p)$  is the spectral ground acceleration at the  $i$ th structural period and at the equivalent damping ratio of the supporting structure,  $\xi_p$ ,  $S_D(T_i, \xi_p)$  is the corresponding spectral displacement,  $m_j$  is the seismic mass at floor  $j$ , and  $\phi_{i,j}$  is the value of the  $i$ th mode shape at floor  $j$ .

In order to evaluate the modal contributions to the peak floor acceleration ( $a_{i,j}$ ) and the peak floor relative displacement ( $\Delta_{R,i,j}$ ) for supporting structures behaving in the nonlinear range, the following effects have to be considered. As the supporting structure yields, its first mode forces saturate and its effective fundamental period lengthens. The forces associated with higher modes keep increasing as seismic intensity increases. On the other hand, the effective period of the higher modes lengthens with increasing seismic intensity because of the decrease in effective stiffness associated to

the first mode.<sup>48,49</sup> The procedure to evaluate  $\Delta_{R1,j}$  is described in detail in Section 4.2. The following equations are suggested to predict the contributions of the first mode to the peak floor acceleration and the peak floor relative displacement:

$$a_{1,j} = \frac{\delta_j}{\sum_{j=1}^n m_j \delta_j} V_b, \quad (28)$$

$$\Delta_{R,1,j} = \frac{\sum_{j=1}^n m_j \delta_j}{\sum_{j=1}^n m_j \delta_j^2} \delta_j \Delta_d, \quad (29)$$

where  $\delta_j$  is the value of the first inelastic mode shape at floor  $j$ ,  $V_b$  is the base shear capacity at the displacement demand on the supporting structure, and  $\Delta_d$  is the displacement demand of the equivalent SDOF system representative of the supporting structure obtained from the process explained in Section 4.2. Note that the contribution of the first mode to the peak floor acceleration of floor  $j$  ( $a_{1,j}$ ) saturates at the acceleration level causing yielding of the supporting structure.<sup>9</sup> Because of this,  $a_{1,j}$  can be estimated by dividing the supporting structure's lateral resistance by the effective mass of the first inelastic mode shape and then distributing it up the height of the structure according to the same mode shape; Equation (28) is obtained as a result of this process.

5. The PGD at the construction site must be estimated in order to obtain the final value of the peak floor absolute displacement from Equations (20) and (21). Estimating the PGD is not a simple issue because of lack of information in modern building codes.<sup>7,8</sup> In the last few years, some significant efforts have been made to reduce the uncertainties related to the estimation of PGD. Recently, Smerzini et al<sup>50</sup> and Faccioli and Villani<sup>51</sup> developed a new procedure for the evaluation of more accurate design response spectra in the European context including probabilistic seismic hazard analysis (PSHA) results at long periods. The use of PSHA results is recommended as a first option in order to obtain FRS with consistent seismic hazard return period for the entire range of nonstructural periods.
6. The  $DAF$  must be computed according to Equations (8) to (10), then the peak floor spectral acceleration can be calculated as follows:

$$S_{AF,max,i,j} = DAF a_{i,j}. \quad (30)$$

7. The parameters gathered in the previous steps are used to compute the contribution of each mode to the relative displacement and absolute acceleration FRS. The following equations are used to predict the relative displacement FRS:

$$S_{DF,i,j}(T_a) = \frac{1}{4\pi^2} \left( \frac{T_a^2}{T_i} \right)^2 (S_{AF,max,i,j} - a_{i,j})g + \frac{T_a^2}{4\pi^2} a_{i,j}g \quad \text{if } T_a \leq T_i, \quad (31)$$

$$S_{DF,i,j}(T_a) = \frac{T_a^2}{4\pi^2} S_{AF,max,i,j} \quad \text{if } T_i < T_a \leq T_{e,i}, \quad (32)$$

$$S_{DF,i,j}(T_a) = \Delta_{ab,i,j} + \left( \frac{T_{e,i}}{T_a} \right)^2 \left( \frac{T_{e,i}^2}{4\pi^2} S_{AF,max,i,j} g - \Delta_{ab,i,j} \right) \quad \text{if } T_a > T_{e,i}. \quad (33)$$

Applying the pseudo-spectral relationship (Equation 16) to the previous three equations, the consistent absolute acceleration FRS can be estimated as follows:

$$S_{AF,i,j}(T_a) = \left( \frac{T_a}{T_i} \right)^2 (S_{AF,max,i,j} - a_{i,j}) + a_{i,j} \quad \text{if } T_a \leq T_i, \quad (34)$$

$$S_{AF,i,j}(T_a) = S_{AF,max,i,j} \quad \text{if } T_i < T_a \leq T_{e,i}, \quad (35)$$

$$S_{AFi,j}T_a = \frac{4\pi^2}{T_a^2 g} \Delta_{ab,i,j} + \frac{4\pi^2}{g} \left( \frac{T_{e,i}}{T_a} \right)^2 \left( \frac{T_{e,i}^2}{4\pi^2} S_{AF, \max,i,j} g - \Delta_{ab,i,j} \right) \text{ if } T_a > T_{e,i}. \quad (36)$$

As with the Sullivan et al<sup>24</sup> methodology described in Section 2.1 for a supporting structure remaining elastic (ie,  $T_{e,i} = T_i$  for all modes), the relative displacement FRS is estimated using only Equations (31) and (33), while the absolute acceleration FRS is estimated using only Equations 34 and 36. The effective period,  $T_{e,i}$ , to be used for the prediction of FRS in supporting structures behaving in the nonlinear range can be estimated according to the following simplified equations:

$$T_{e,i} = T_i \sqrt{\mu} \quad \text{if } i \leq 2, \quad (37)$$

$$T_{e,i} = T_i \quad \text{if } i > 2. \quad (38)$$

Equation 37 implies that the second mode period elongates as much as the first mode period when the ductility demand increases. Although in reality the second mode of RC frames does not experience so much elongation, Equation (37) is deemed conservative and in good agreement with the results obtained in this study. Additionally, no detailed studies exist that quantify the expected lengthening of higher modes in frame structures (some information exists for cantilever structures<sup>26,48,49</sup>). Equations (37) and (38) are intended only for RC supporting structures; for steel supporting structures, better modelled by an elastic perfectly plastic behavior, period lengthening in FRS is often not observed and  $T_{e,i} = T_i$  for all modes.<sup>20,26</sup> One alternative to Equations (37) and (38) to find the effective periods of higher modes is to perform an elastic eigenvalue analysis with the initially cracked stiffness properties of the plastic hinge locations divided by the ductility demand  $\mu$ .<sup>10</sup>

8. Finally, the contributions of each mode are combined through SRSS. Note that by applying the SRSS combination of the individual modal contributions to the FRS, the limiting value at very long periods of the final estimate of the FRS is the peak floor absolute displacement predicted by Equation (19). For the floors in the lower half of the building, the envelope between the ground spectrum and the SRSS combination of each mode should be used as a final estimate. Furthermore, for periods beyond the fundamental period of the supporting structure, it is recommended that the envelope of the ground spectrum and the SRSS combination of the individual modes be considered for all floors. This last point is necessary to account for the possible amplification of the response of the supporting structure because of long-period seismic waves.

## 5 | APPRAISAL OF PROPOSED METHODOLOGY THROUGH NLTH ANALYSES

The archetype RC frames were analyzed using NLTH analyses for both the 70- and 2475-year ground motions. The FRS computed from NLTH analyses are compared with the FRS predicted by the proposed methodology described in Section 4.3 as well as by the methodology proposed by Vukobratović and Fajfar.<sup>23,39</sup> The comparison is presented in ADRS format assuming a 5.0% nonstructural damping ratio ( $\xi_a = 0.05$ ). Relative displacement FRS are also compared on a linear period scale. The median ground spectra obtained from the two ground motion ensembles (Figure 5A,B) were used to define the input parameters required to apply the simplified procedures. The PGD was taken as the median from the displacement time histories of the same records.

Figure 8 shows the comparison of FRS for three representative floors (first, mid-height, and top) of the two-, four-, and eight-story archetype frames under the 70-year ground motions. A good agreement between the median spectral values obtained from NLTH analyses and those predicted by the proposed methodology is observed for all three archetype RC frames. The peak spectral absolute accelerations and relative displacements at the fundamental periods of the supporting structures are predicted reasonably well with peak spectral relative displacements at the first period slightly underestimated at some floors. For the two-story RC frame, the proposed methodology produces un-conservative estimates of the spectral displacements for periods longer than 1.5 seconds. The worst predictions were observed at the first floors, due, again, to the strong influence of the ground motions. The mean absolute error between the predicted spectral absolute accelerations and spectral relative displacements and those obtained from the NLTH analyses, evaluated

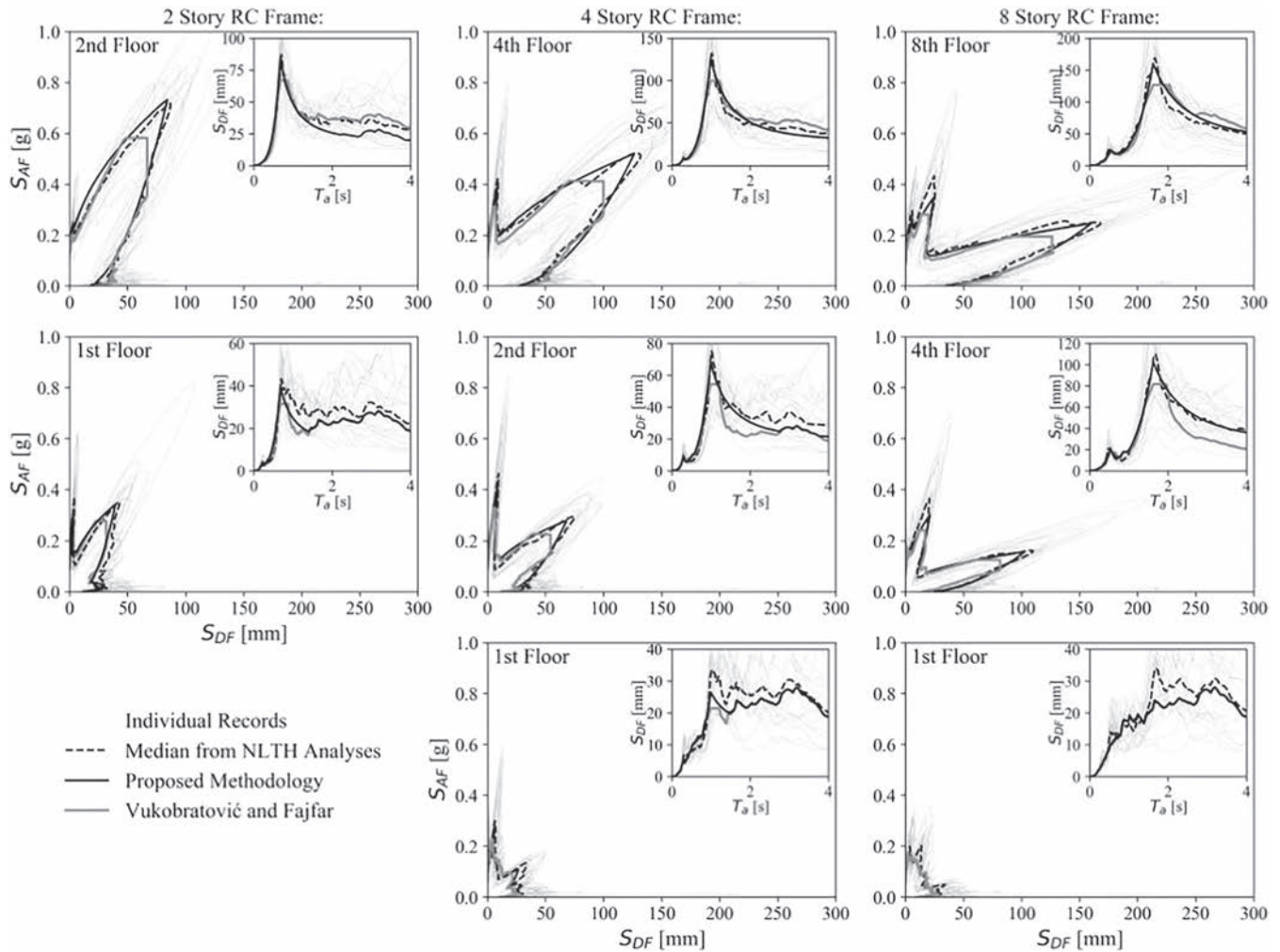


**FIGURE 8** Comparison between the FRS obtained from NLTH analyses and the predictions made by the proposed methodology and the Vukobratović and Fajfar methodology for the two, four and eight-story archetype RC frames (each in one column) under 70-year ground motions. FRS, floor response spectra; NLTH, nonlinear time-history; RC, reinforced concrete

across all archetype frames, for nonstructural periods up to 3.0 seconds, are equal to 15.9 % and 15.3 %, respectively. These results demonstrate the adequate prediction capability of the proposed simplified methodology. Note that the general shape of the FRS is well predicted also in the off-resonance regions. Comparing the results obtained from NLTH analyses with those predicted by the Vukobratović and Fajfar methodology, a good match is observed in terms of shape of the FRS. The peak absolute accelerations and relative displacements are often under predicted, probably due to the broadening of the peaks in the absolute acceleration and relative displacement FRS. For nonstructural periods longer than the fundamental period of the supporting structure, the prediction capability of the Vukobratović and Fajfar methodology is lower for intermediate floors (second floor of the four-story RC frame and fourth floor of the eight-story frame). Note that the introduction of a lower limit represented by the ground spectrum<sup>39</sup> improves considerably the match with the results of the NLTH analyses for the bottom floors of the analyzed frames but not for the other floors in the lower half of the analyzed buildings.

Figure 9 compares the FRS for the 2475-year ground motions. As for the 70-year ground motions, the proposed methodology provides good estimations of the absolute acceleration and relative displacement FRS. Both the FRS shapes and the peak spectral absolute accelerations and relative displacements at the fundamental periods of the supporting structures are well predicted. Similar to the 70-year ground motions case, the mean absolute errors are 15.8% and 16.0% for spectral accelerations and displacements, respectively. The predictions are generally conservative for most of the nonstructural period range, with few exceptions for longer periods (longer than 3.0 s), and at the lowest floors. For the two-story frame, un-conservative predictions can be observed for period longer than 1.5 seconds. The slightly un-conservative results at very long nonstructural periods are probably due to the long-period seismic waves of the ground

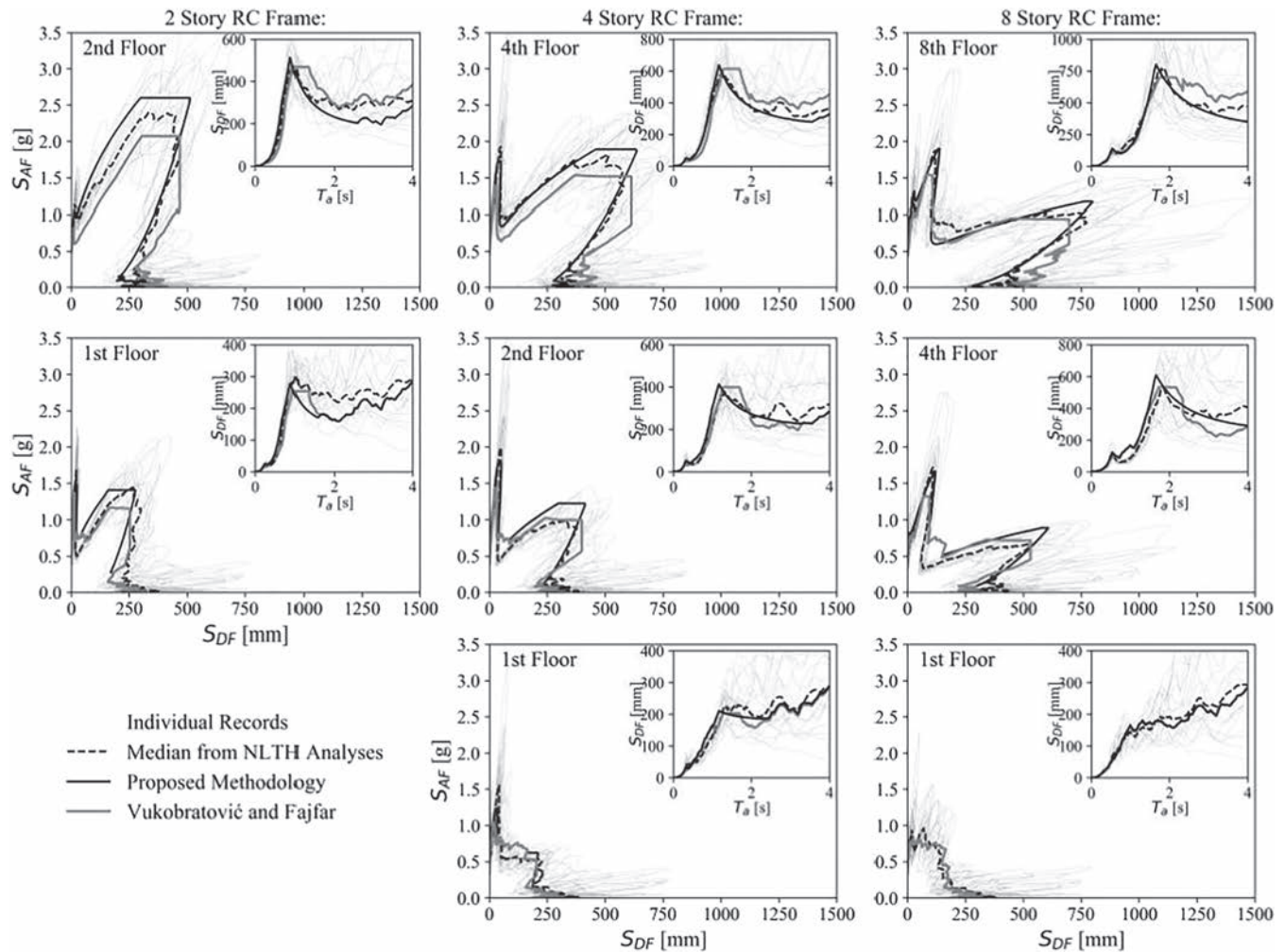


**FIGURE 9** Comparison between the FRS obtained from NLTH analyses and the predictions made by the proposed methodology and the Vukobratović and Fajfar methodology for the two-, four-, and eight-story archetype RC frames (each in one column) under 2475-year ground motions. FRS, floor response spectra; NLTH, nonlinear time-history; RC, reinforced concrete

motion itself. If the corner period of the ground motions is longer than the fundamental period of the supporting structure, many of the seismic waves in the constant displacement region of the ground spectrum could be amplified by the structure. It is unlikely that NSEs would have effective periods longer than 3.0 seconds. The same considerations pointed out for the 70-year ground motions can be extended to the 2475-year ground motions for the methodology proposed by Vukobratović and Fajfar. A good match in the shape of the FRS is generally observed; the peaks of the absolute acceleration and relative displacement FRS are underestimated in some cases, despite the comparison being improved with respect to the 70-year ground motions. For the RC frames with more significant nonlinear response (two- and four-story RC frames), the procedure produces slightly un-conservative spectral acceleration and displacement values at the top story for nonstructural periods shorter than the fundamental period of the supporting structure; this is likely due to the fact that the effective period is used in Equations (11) through (15) when the supporting structure experiences nonlinear response. For nonstructural periods longer than the fundamental period of the supporting structure, the procedure predicts conservative results at the top floors of all the RC frames and un-conservative results for the fourth floor of the eight-story RC frame.

## 6 | CONCLUSIONS

The seismic design and assessment of NSEs require the accurate estimation of the seismic demand through the prediction of FRS. The definition of consistent absolute acceleration and relative displacement FRS is the most suitable approach to gain all the information required for the design of many typologies of NSEs. This study modified an existing

methodology to predict absolute acceleration FRS to provide consistent estimates of relative displacement FRS. The main findings of the study are listed below:

1. A simple correction procedure was proposed herein to modify the Sullivan et al procedure<sup>24-26</sup> in order to predict consistent absolute acceleration and relative displacement FRS. The modified procedure applies both to supporting structures subjected to low and medium-high seismic intensities. For the latter intensity, a nonlinear response can be expected.
2. The modified approach relies on the physical requirement that at very long nonstructural periods, the relative displacement of the NSEs converges to the peak absolute displacement of the floor on which they are supported.
3. A simplified procedure for estimating the peak floor absolute displacement was proposed. This simplified approach estimates the peak floor absolute displacement through the SRSS combination of the modal contributions to the peak floor relative displacement and the PGD at the site of interest. For the archetype RC frames of various heights considered in this study, the peak floor absolute displacements predicted by the simplified approach were in good agreement with those obtained from time-history analyses.
4. The effectiveness of the proposed procedure, for estimating both absolute acceleration and relative displacement FRS, was assessed through the results of dynamic NLTH analyses on the four archetype RC frames. The peak spectral absolute accelerations and relative displacements, as well as the general shape of the FRS, were well predicted both for 70- and 2475-year ground motions. The proposed methodology allows to predict reasonably well consistent FRS for NSE periods longer than the fundamental period of the supporting structure, with some discrepancies only for nonstructural periods longer than 3.0 seconds. It is unlikely that NSEs would exhibit such long periods.

The proposed methodology provides an effective tool for the prediction of the seismic demand on NSEs and for the application of a recently developed DDBD procedure of NSEs, which requires the estimation of relative displacement FRS. The proposed methodology should, however, be further assessed for a variety of supporting structural typologies responding both in the linear and nonlinear ranges. Furthermore, the proposed methodology should be also validated for other locations where the seismic demand on the supporting structure is expected to be higher (eg, western coast of the United States) with a more pronounced nonlinear response of the supporting structure.

## ACKNOWLEDGEMENTS

The work presented in this paper has been developed within the framework of the project “Dipartimenti di Eccellenza,” funded by the Italian Ministry of Education, University and Research at IUSS Pavia. The EUCENTRE Foundation is gratefully acknowledged for provided financial support to the first author of this paper. The authors gratefully acknowledge also the Italian Department of Civil Protection (DPC) for their financial contributions to this study through the ReLUIS 2019-2021 Project (Work Package 17 - Contributi Normativi Per Elementi Non Strutturali).

## ORCID

Roberto J. Merino  <https://orcid.org/0000-0002-1116-468X>

Daniele Perrone  <https://orcid.org/0000-0001-9080-2215>

## REFERENCES

1. Miranda E, Mosqueda G, Retamales R, Pekcan G. Performance of nonstructural components during the 27 February 2010 Chile Earthquake. *Earthq Spectra*. 2012;28(S1):S453-S471.
2. Perrone D, Calvi PM, Nascimbene R, Fischer E, Magliulo G. Seismic performance and damage observation of non-structural elements during the 2016 Central Italy Earthquake. *Bull Earthquake Eng*. 2018;17(10):5655-5677. <https://doi.org/10.1007/s10518-018-0361-5>
3. Dhakal RP. Damage to non-structural components and contents in 2010 Darfield earthquake. *Bull New Zeal Soc Earthquake Eng*. 2010;43(4):404-411.
4. O'Reilly GJ, Perrone D, Fox M, Monteiro R, Filiatrault A. Seismic assessment and loss estimation of existing school buildings in Italy. *Eng Struct*. 2018;168(1):142-162.
5. Sousa L, Monteiro R. Seismic retrofit options for non-structural building partition walls: Impact on loss estimation and cost-benefit analysis. *Eng Struct*. 2018;161:8-27.

6. FEMA. *P-58, Seismic Performance Assessment of Buildings*. Washington, DC: Federal Emergency Management Agency; 2012.
7. ASCE. *Minimum design loads for buildings and other structures, ASCE/SEI Standard 7-16*. Reston: American Society of civil engineers; 2016.
8. CEN. *Eurocode 8 – Design provisions for earthquake resistant structures, EN-1998-1:2004*. Brussels, Belgium: Comite Europeen de Normalization; 2004.
9. Filiatrault A, Perrone D, Merino RJ, Calvi GM. Performance-based seismic design of non-structural building elements. *J Earthquake Eng*. 2018;n/a:1-33. <https://www.tandfonline.com/doi/full/10.1080/13632469.2018.1512910?scroll=top&edAccess=true>
10. Priestley MJN, Calvi GM, Kowalsky MJ. *Displacement-based seismic design of structures*. Pavia, Italy: IUSS Press, Istituto Universitario di Studi Superiori di Pavia; 2004.
11. Lin J, Mahin S. Seismic response of light subsystems on inelastic structures. *J Struct Eng*. 1985;111(2):400-417.
12. Sewell RT, Cornell CA, Toro GR, McGuire RK, Kassawara RP, Sing A. Factors influencing floor response spectra in nonlinear multi-degree-of-freedom structures, *Report N082*, Stanford University, 1988.
13. Medina R, Sankaranarayanan R, Kingston KM. Floor response spectra for light components mounted on regular moment-resisting frame structures. *Eng Struct*. 2006;28(14):1927-1940.
14. Sankaranarayanan R, Medina R. Acceleration response modification factors for nonstructural components attached to inelastic moment-resisting frame structures. *Earthquake Eng Struct Dynam*. 2007;36(14):2189-2210.
15. Chaudhuri S, Villaverde R. Effect of building nonlinearity on seismic response of nonstructural components: a parametric study. *J Struct Eng*. 2008;134(4):661-670.
16. Chaudhuri S, Hutchinson T. Distribution of peak horizontal floor acceleration for estimating nonstructural element vulnerability, *Proceeding of 13th World conference on Earthquake engineering*, Paper n.1721, Vancouver, Canada, 2004.
17. Miranda E, Taghavi S. Approximate floor acceleration demands in multistorey building. I: formulation. *J Struct Eng*. 2005;131(2):203-211.
18. Singh M, Moreschi L, Suarez L, Matheu E. Seismic design forces II: flexible nonstructural components. *J Struct Eng*. 2006;132(10):1533-1542.
19. Singh M, Moreschi L, Suarez L, Matheu E. Seismic design forces I: rigid nonstructural components. *J Struct Eng*. 2006;132(10):1524-1532.
20. Politopoulos I, Feau C. Some aspects of floor spectra of 1DOF nonlinear primary structures. *Earthquake Eng Struct Dynam*. 2007;36:975-993.
21. Politopoulos I. Floor spectra of MDOF nonlinear structures. *J Earthquake Eng*. 2010;14(4):726-742.
22. Petrone C, Magliulo G, Manfredi G. Seismic demand on light acceleration-sensitive nonstructural components in European reinforced concrete buildings. *Earthquake Eng Struct Dynam*. 2015;8(10):1203-1217.
23. Vukobratović V, Fajfar P. Code-oriented floor acceleration spectra for building structures. *Bull Earthquake Eng*. 2017;15:3013-3026.
24. Sullivan TJ, Calvi PM, Nascimbene R. Towards improved floor spectra estimates for seismic design. *Earthquake Struct*. 2013;4(1):109-132.
25. Calvi PM, Sullivan TJ. Estimating floor spectra in multiple degree of freedom systems. *Earthquake Struct*. 2014;7(1):17-38.
26. Welch DP, Sullivan TJ. Illustrating a New Possibility for the Estimation of Floor Spectra in Nonlinear Multi-Degree of Freedom Systems. *Proceedings of the 16th World Conference on Earthquake, 16WCEE*, Paper N° 2632, Santiago, Chile, 2017.
27. Obando JC, Lopez-Garcia D. Inelastic displacement ratios for nonstructural components subjected to floor accelerations. *J Earthquake Eng*. 2016;22(4):569-594.
28. Calvi PM. Relative displacement floor spectra for seismic design of non structural elements. *J Earthquake Eng*. 2014;18(7):1037-1059.
29. FEMA. *Reducing the risks of nonstructural earthquake damage—a practical guide*. FEMA E-74, Federal Emergency Management Agency and National Earthquake Hazard Reduction Program, USA, 2012.
30. Gabbianelli G, Kanyilmaz A, Bernuzzi C, Castiglioni CA. A combined experimental-numerical study on unbraced pallet rack under push-over loads. *Ingegneria Sismica*. 2017;34(1):18-38.
31. Koliou M, Filiatrault A, Reinhorn AM. Seismic response og high-voltage transformer-bushing systems incorporating flexural stiffeners II: Experimental study. *Earthq Spectra*. 2013;29(4):1353-1367.
32. NIST GCR 18-917-43. *Recommendations for improved seismic performance of nonstructural elements*. Applied Techonology Council, CA, 2018.
33. Brandolese S, Fiorin L, Scotta R. Seismic demand and capacity assessment of suspended ceiling systems. *Eng Struct*. 2019;193:219-237.
34. Vukobratović V, Fajfar P. A method for the direct determination of approximate floor response spectra for SDOF inelastic structures. *Bull Earthq Eng*. 2015;13(5):1405-1424.
35. Vukobratović V, Fajfar P. A method for the direct estimation of floor acceleration spectra for elastic and inelastic MDOF structures. *Earthq Eng Struct Dyn*. 2016;45(15):2495-2511.
36. Filiatrault A, Tremblay R, Christopoulos C, Folz B, Pettinga D. *Elements of Earthquake Engineering and Structural Dynamics*. Third ed. Montreal, Canada: Polytechnic International Press; 2013:874.
37. Fajfar P. A nonlinear analysis method for performance-based seismic design. *Earthq Spectra*. 2000;16:573-592.

38. Yasui Y, Yoshihara T, Takeda T, Miyamoto A. Direct generation method for floor response spectra, *Proceedings of the 12th International Conference on Structural Mechanics in Reactor Technology*, Stuttgart, Germany, 1993.
39. Fajfar P, Faculty of Civil and Geodetic Engineering, University of Ljubljana. Ljubljana, Slovenia. Personal Communication, 2019.
40. USNRC. Regulatory guide 1.22 Development of floor design response spectra for seismic design of floor-supported equipment or components, *U.S. Nuclear Regulatory Commission Office of Standards Development*, 1978.
41. Perrone D, Brunesi E, Filiatrault A, Nascimbene R. Probabilistic estimation of floor response spectra in masonry infilled reinforced concrete building portfolio, *Engineering Structures*. 2019;202:109842
42. NTC08. Nuove norme tecniche per le costruzioni. D.M. Infrastrutture, 2008
43. Mazzoni S, McKenna F, Scott M H, Fenves G L. OpenSees Command Language Manual, *Pacific Earthquake Engineering Research Center*, Berkeley, California, 2006.
44. PEER NGA-West database, available on-line: <http://peer.berkeley.edu/ngawest>
45. Jayaram N, Lin T, Baker JW. A computationally efficient ground-motion selection algorithm for matching a target response spectrum mean and variance. *Earthq Spectra*. 2011;27(3):797-815.
46. Welch DP, Sullivan TJ, Calvi GM. Developing Direct Displacement-Based procedures for simplified loss assessment in performance-based earthquake engineering. *J Earthquake Eng*. 2014;18(2):290-322.
47. Dwairi HM, Kowalsky MJ, Nau JM. Equivalent damping in support of direct displacement-based design. *J Earthquake Eng*. 2007;11(4):512-530.
48. Wiebe L, Christopoulos C. A cantilever beam analogy for quantifying higher mode effects in multistory buildings. *Earthquake Engng & Struct Dyn*. 2015;44:1697-1716.
49. Pennucci D, Sullivan TJ, Calvi GM. Inelastic higher-mode response in reinforced concrete wall structures. *Earthq Spectra*. 2015;31(3):1493-1514.
50. Smerzini C, Galasso C, Iervolino I, Paolucci R. Ground motion record selection based on broadband spectral compatibility. *Earthq Spectra*. 2014;30(4):1427-1448.
51. Faccioli E, Villani M. Seismic hazard mapping for Italy in terms of broadband displacement response spectra. *Earthq Spectra*. 2009;25(3):515-539.

**How to cite this article:** Merino RJ, Perrone D, Filiatrault A. Consistent floor response spectra for performance-based seismic design of nonstructural elements. *Earthquake Engng Struct Dyn*. 2020;49:261–284. <https://doi.org/10.1002/eqe.3236>